Article

Not peer-reviewed version

Yeast Culture Modulates Colonic Microbiota and Immune Barrier to Mitigate High-Concentrate Diet–Induced Stress in Sheep

Haoke Li , Mingqiang Niu , Jinping Shi , Zhixiong Tang , Feifei Yang , Zhengwu Pi , Shuru Cheng *

Posted Date: 9 March 2026

doi: 10.20944/preprints202603.0537.v1

Keywords: sheep; colon; yeast culture; VFAs; microorganisms

 doi:10.20944/preprints202603.0537.v1

Article

Yeast Culture Modulates Colonic Microbiota and Immune Barrier to Mitigate High-Concentrate Diet–Induced Stress in Sheep

Haoke Li [1], Mingqiang Niu [2], Jinping Shi [3], Zhixiong Tang [1], Feifei Yang [1], Zhengwu Pi [1] and Shuru Cheng [1,*]

[1] College of Animal Science and Technology, Gansu Agricultural University, Lanzhou 730070, China

[2] College of Veterinary Medicine, Gansu Agriculture University, Lanzhou 730070, China

[3] School of Animal Science and Technology, Ningxia University, Yinchuan, Ningxia Hui Autonomous Region, P. R. China 750021

* Correspondence: chengsr@gsau.edu.cn; Tel: +86-139-1927-0737

Abstract

Objective: To investigate the effects of yeast extract on colonic damage in sheep caused by high-concentrate diets, providing a theoretical basis for developing more precise probiotic formulations. **Methods:** This study selected 45 three-month-old Du Han F1 sheep of similar body condition and randomly divided them into three groups: a control group (CON) fed a standard diet, a high-concentrate diet (HC) group, and a yeast culture treatment group. A 15-day pretrial period was followed by a 60-day main trial. Following the feeding trial, colonic contents and colonic tissue samples were collected. **Results:** Indicate that feeding a high-concentrate diet caused damage to both the colonic mucosa and muscularis layers. Compared with the control group (CON), the high-concentrate diet (HC) group presented 29 DEGs. Following the addition of yeast culture (YC), the number of differentially expressed genes increased to 683, among which 6 were YC-specific genes. Eight differentially abundant bacterial genera were identified: increased abundance of *[Eubacterium]-xylanophilum-group*, *Alistipes*, *Gastranaerophilales*, *Lachnospiraceae-UCG-010*, and *Cyanobacteria*; decreased abundance of *Ruminococcaceae;uncultured*, *Akkermansia*, and *Verrucomicrobiota*. Concurrently, VFA levels decreased while ammonia nitrogen levels increased, accompanied by abnormal expression of host immune barrier-related genes (e.g., *CLDN1*, *CXCL8*). In the HCY group, colonic mucosal integrity improved, microbial composition underwent significant changes, VFA levels rebounded, and ammonia nitrogen levels decreased. **Conclusions:** This indicates that YC modulates the "microbiota-VFA-host" axis network to a certain extent.

Keywords: sheep; colon; yeast culture; VFAs; microorganisms

Introduction

High-concentrate diets, rich in nutrients and energy, rapidly replenish animals' energy and protein requirements, promoting growth and enhancing production performance.Therefore, it is primarily used for fattening. However, with the development of intensive farming, the proportion of high-concentrate diets in sheep rations has increased, readily resulting in subacute ruminal acidosis (SARA). This leads to impaired ruminal fermentation and gastrointestinal dysfunction [1]. During SARA, volatile fatty acids (VFAs) and lactic acid accumulate in rumen contents, pH levels decrease significantly, and microbial diversity decreases, leading to metabolic disorders and weakening the absorptive barrier function of the rumen epithelium [2]. Large amounts of lactic acid and endotoxins (primarily lipopolysaccharides [LPS] from gram-negative bacteria) migrate from the rumen to peripheral tissues, triggering systemic inflammatory responses [3]. This subsequently leads to an imbalance in the host-microbiota equilibrium of the hindgut. Studies indicate that under SARA

 doi:10.20944/preprints202603.0537.v1

conditions, elevated levels of LPS and the pro-inflammatory cytokine tumor necrosis factor-α (TNF-α) are detected in sheep blood and tissues. Significant activation of TLR4 receptors and the NF-κB signaling pathway occurs in tissues, accompanied by abnormal expression of tight junction proteins, leading to an impaired mucosal barrier [3]. Disruption of the intestinal barrier allows pathogenic bacteria and their toxins to readily penetrate the intestinal mucosa, triggering excessive mucosal immune activation and chronic inflammation, thereby exacerbating metabolic stress in the body [4]. Therefore, under a high-concentrate diet feeding regimen, sheep intestines are prone to a vicious cycle of acidosis, barrier damage, and microbial community disruption, severely impacting animal health and production performance.

Current research predominantly focuses on the effects of high-concentrate diets on the rumen and small intestine, with limited investigation into the hindgut. The colon exhibits highly complex and diverse structural, functional, and internal environmental characteristics, posing significant challenges for disease diagnosis and treatment. Within the colon, approximately 17% of digestible fiber undergoes microbial fermentation, producing substantial amounts of volatile fatty acids (VFAs) such as acetate, propionate, and butyrate, which provide a vital supplementary energy source for the host [5]. Moreover, an intact colonic mucosal barrier helps prevent the transmural transfer of harmful microbial metabolites (e.g., endotoxins), thereby safeguarding intestinal and systemic health [6]. Over 70% of the body's immune cells reside within the sheep colon and primarily functioning to maintain tolerance toward commensal microorganisms while preventing pathogen invasion. This critical equilibrium is disrupted during dietary acidosis. High-concentrate diets can damage the hindgut barrier in sheep, triggering mucosal inflammation. In a trial involving Hu sheep, high-concentrate diets reduced expression of the goblet cell mucoprotein MUC2 and tight junction proteins, impairing colonic barrier function. This was accompanied by marked inflammation and tissue thickening in the colonic mucosa [7]. These findings demonstrate that under normal conditions, the colonic barrier provides a physiological advantage against the leakage of pro-inflammatory substances into the systemic circulation. Its impairment leads to inflammatory responses in the sheep colon and compromised health.

Yeast culture (YC), a microbial fermentation product, is widely used in ruminant diets to alleviate gastrointestinal disorders caused by dietary imbalances [8]. Yeast culture is typically obtained through the complete fermentation of yeast on specific media, comprising extracellular metabolites of yeast cells, transformed fermentation medium, and a small amount of inactivated yeast cells [9]. Research indicates that adding yeast culture stabilizes rumen fermentation, enhances nutrient digestibility, and modulates immune responses to some extent [10]. Concurrently, YC indirectly reduces hindgut acid load and barrier damage risk by stabilizing ruminal fermentation and pH levels [11].

Research on the effects of high-concentrate diets on sheep colonic microbiota and barrier function remains limited, and the mechanism of yeast culture intervention is unclear. Therefore, this study selected Duhan crossbred sheep as experimental subjects to investigate the potential impacts of high-concentrate diets on sheep and the intervention mechanism of yeast culture, aiming to achieve synergistic optimization of efficient feeding and animal health in sheep.

Materials and Methods

Feeding Trial and Sampling

This study employed a randomized design using individual animals as experimental units. Forty-five healthy, similar-condition 3-month-old Duhan crossbred rams were randomly assigned to 45 separate pens and fed according to their respective groups. The treatment groups were designed as follows: (1) Control group (CON); (2) High-concentrate diet group (HC); (3) Yeast Culture Treatment Group (Xi'an Xinhanbao Biotechnology Co., Ltd.) fed (HCY). The feed formulation is shown in Table 1 (inactive yeast). Water was provided ad libitum. After 60 days of feeding, five healthy sheep were randomly selected from each group and transported to a local slaughterhouse for slaughter upon trial completion. Five milliliters of the colonic contents were collected into cryogenic

 doi:10.20944/preprints202603.0537.v1

tubes, rapidly frozen in liquid nitrogen, and stored at -80 °C for microbiome analysis and VFA determination. The colon walls were then gently rinsed with sterile saline to remove residual contents. Two tissue samples were obtained: one fixed was in 4% paraformaldehyde solution at 4 °C for histological sectioning; and the other was stored in an RNA preservative (RNAlater) at -80℃ for RNA extraction.

Table 1. Compositions and nutrient levels of the diets (DM basis).

Items (%)	Groups		
	CON	HC	HCY
Corn	20.96	36.29	36.29
Soybean hull	18.7	15.8	15.5
Spray-coated corn husk	15.5	15	15
Corn germ meal	13.5	7.9	7.9
Rice hull powder	7.6	5	5
Flour	7	10.5	10.5
Bran	4.2		
Stone powder	2.64	2.51	2.51
Soybean meal		2.5	2.5
Rice bran	2.3		
Pumpkin seed hull	2.1		
Sugarcane molasses	2	2	2
Bentonite	1		
Expanded urea[1]	1	1	1
Sodium chloride	0.5	0.5	0.5
Yeast culture			0.3
1% premix[1]	1.	1	1
Chemical composition, % of DM			
DM	89.58	88.72	88.72
CP	14.90	14.91	14.92
EE	3.25	2.52	2.52

 doi:10.20944/preprints202603.0537.v1

Starch-Ew	25.99	34.96	34.98
NDF	31.83	25.07	25.07
ADF	11.77	12.58	12.58
Ca	1.20	1.10	1.10
P-total	0.40	0.35	0.35

1) The premix provided the following per kg of diet:VA 15 000 IU, VD 2 200 IU, VE 50 IU, Fe 55 mg, Cu 12.5 mg, Mn 47 mg, Zn 24 mg, Se 0.5 mg, I 0.5 mg, Co 0.1 mg.

Hematoxylin and Eosin (H&E) Staining

Fixed colon samples were retrieved, subjected to routine dehydration, cleared, paraffin embedded, and sectioned into 4 μm-thick slices. After xylene dewaxing and gradient ethanol hydration, the sections were stained with hematoxylin for 5–8 minutes. Following differentiation with 1% hydrochloric acid ethanol and counterstaining with water, the sections were counterstained with 0.5% eosin solution for 1–3 minutes. The sections were then dehydrated with graded ethanol, cleared with xylene, and finally sealed with neutral resin. Histological structures were examined under a microscope to assess intestinal barrier integrity.

16. S rRNA Amplification and Sequencing

Total DNA was extracted from each sample using magnetic bead technology (100–200 mg fecal sample was mixed with lysis buffer, Proteinase K, and 1 mm grinding beads, homogenized by mechanical disruption, and lysed at 70 °C). After centrifuging the lysis buffer and collecting the supernatant, RNase A and binding buffer were sequentially added. Following centrifugation to remove impurities, the supernatant was transferred to a DNA binding column for binding. Subsequently, the sample was washed sequentially with wash buffers to remove residual impurities and salts. Finally, elution with TE buffer or nuclease-free water yielded fecal genomic DNA, with DNA concentration, purity, and integrity subsequently assessed. Barcoded primers were synthesized targeting the 341F (CCTACGGGNGGCWGCAG) and 806R (GGACTACHVGGGTWTCTAAT) regions for PCR amplification. Amplified products were purified and sequenced using paired-end (PE250) read lengths on an Illumina MiSeq platform. Raw sequencing reads underwent quality control using Trimmomatic to remove adapter sequences, low-quality bases, and N-containing reads. Subsequently, paired-end reads were assembled using FLASH or PEAR based on read overlap, with a minimum overlap length of 10 bp and a maximum mismatch rate of 0.1. Chimeric sequences were removed from Fasta files using the Uchime method against known databases. For unknown databases, chimeras were eliminated via self-alignment (Denovo) alongside short sequences failing quality thresholds. Clean Tags were then subjected to bioinformatics analysis using the Uparse clustering method to generate OTUs at 97% similarity. OTU-based species annotation (using Silva128 as reference database), diversity analysis, and differential analysis were subsequently performed. Functional prediction of microbial communities was performed using PICRUSt2 software based on 16S rRNA sequencing data. Significantly altered metabolic pathways were identified via LEfSe (LDA > 2.0, $P < 0.05$), providing insights into potential metabolic functional impacts of microbial community shifts. Due to limitations in functional prediction, results serve only as supplementary interpretation.

Transcriptome Sequencing to Observe the Molecular Effects of the Microbiota on the Gut

Total RNA was extracted from 15 colon samples via an appropriate volume of TRIzol reagent. The RNA integrity and concentration were assessed via a bioanalyzer (Agilent Bioanalyzer 2100 system). Following cDNA library construction, high-throughput transcriptome sequencing was

 doi:10.20944/preprints202603.0537.v1

performed via the MGI sequencing platform to obtain raw data. High-quality data (clean reads) were filtered and aligned to the sheep genome ARS-UI_Ramb_v3.0 via HISAT2 alignment software. Transcriptome assembly was then performed via stringtie. New transcripts were identified by comparing the assembly with existing annotations via cuffcompare. CPC was subsequently employed to predict the protein-coding potential of these new transcripts. TransDecoder was then used to predict coding regions for transcripts with protein-coding potential, yielding new genes with coding capacity. These new genes were then integrated into the reference gene set. Finally, quantitative analysis of the integrated gene set was performed via RSEM. Differential gene expression analysis was conducted with the DESeq2 package, setting thresholds at $|\log2 \text{ Fold Change}| > 0.58$ and FDR-adjusted $P < 0.05$. The DEGs were subjected to Kyoto Encyclopedia of Genes and Genomes (KEGG) analysis to screen for genes associated with the immune response and barrier function pathways, and differences in gene expression were observed.

GC Targeted Detection of VFAs

Detection was performed via an Agilent 8890 GC gas chromatograph. A 5 mL filtrate was centrifuged at 4,000 r/min for 15 min. One milliliter of the supernatant was then mixed with 25% metaphosphoric acid solution at a 4:1 ratio. After mixing for 30 min in an ice–water bath, the mixture was centrifuged at 4,000 r/min for 15 min in a 4 °C centrifuge. The filtrate was transferred into dedicated vials. The operating conditions for the gas chromatograph were as follows: FFAP column, 30 m × 0.32 mm × 0.25 μm. The forward injection port with an injector heater set to 300 °C and a split ratio of 10:1 was used. The column temperature was as follows: initial temperature of 80 °C held for 1 min; ramped at 10 °C/min to 170 °C, held for 1 min; and continued at 20 °C/min to 250 °C, held for 5 min, with a maximum column oven temperature of 300 °C. Hydrogen flame ionization detection (FID) was employed with nitrogen as the carrier gas; the detector heater temperature was 300 °C, the injection volume was 1 μL, and the run time was 20 min. 2-Ethylbutyric acid served as the internal standard.

Determination of Ammonia Nitrogen

Take 10 mL of colonic contents and centrifuge at 3500–4000 rpm for 10 minutes. Measure 2 mL of supernatant (if ammonia nitrogen content is high, take 1 mL supernatant and add 1 mL distilled water), place in a 15 mL test tube, then add 8 mL of 0.2 mol/L hydrochloric acid to a final volume of 10 mL and mix thoroughly. Prepare standard solution, stock solution (dissolve 0.382 g ammonium chloride in 0.2 mol/L hydrochloric acid and dilute to 100 mL), and working solution (take 10 mL stock solution and dilute with distilled water to 100 mL) sequentially. Sequentially measure 0, 1, 2, 4, and 6 mL of the working solution into five labeled 50 mL volumetric flasks. Add distilled water to each to a final volume of 10 mL, then add Solution A (0.08 g Na_2 $[Fe(CN)_5NO]\cdot 2H_2O$ dissolved in 100 mL of 14% $NaC_6H_4(OH)CO_2$ solution) and Solution B (2 mL NaClO mixed into 100 mL of 0.3 M NaOH solution), then add 0.2 mol/L hydrochloric acid to the mark. Measure the absorbance using a 721 spectrophotometer. Measure at 700 nm using a 0.5 cm cuvette. Use nitrogen-free blank solution (No. 0 tube) as the blank control. Record the absorbance values for each sample. Calculate the ammonia nitrogen content using the standard curve equation..

qPCR Validation

To validate the reliability of RNA-Seq results, we selected key differentially expressed genes and performed qPCR validation using the same colon RNA samples (n=5 per group) as those used for transcriptome sequencing. Colonic RNA was extracted from each group, reverse transcribed into cDNA, and amplified using specific primers targeting the genes of interest. Expression levels were compared to the housekeeping gene (*GAPDH*) and calculated as relative expression (using the $2^{-\Delta\Delta Ct}$ method). qPCR results generally aligned with sequencing trends, confirming the accuracy and

 doi:10.20944/preprints202603.0537.v1

reliability of the transcriptomic analysis. Primer sequences are listed below, synthesized by Wuhan Savier Biotechnology Co., Ltd.:, are listed below Table 2.

Table 2. List of primer sequences for quantitative real-time PCR.

Gene	GeneBank accession no.	Direction	Primer sequence (5′–3′)	Length (bp)
CXCL8	NM_001009401.2	Forward	AACACATTCCACACCTTTCCACC	173
		Reverse	CTCTCTTCAAAAATGCCTGCACA	
IL23A	NM_001185122.2	Forward	GGGAACAGAGTTGTGATGCT	164
		Reverse	TCCACATGTCCCATTGGTAGG	
Ovar-DRB1	NM_001280698.2	Forward	CTGTATTTCTCCAGAGGCTCCC	124
		Reverse	GACACTCGCTCTTAGCATACTCC	
CLDN1	NM_001185016.1	Forward	AAGACGACGAGGCACAGAAGA	168
		Reverse	GAGCCTGACCAAATTCATACCTG	
ADIPOQ	NM_001308565.1	Forward	TTCCACACCTGAGGGACTC	136
		Reverse	AATGCCTGCCATCCAACCTG	
GAPDH	NM_001190390.1	Forward	GTCAAGGCAGAGAACGGGAA	106
		Reverse	CGTACTCAGCACCAGCATCA	

Western Blot Validation of Relevant Protein Expression Levels

All operations were performed on ice. Approximately 20 mg of colon tissue was lysed thoroughly with RIPA lysis buffer. The lysate was centrifuged at 4 °C and 12,000 r/min for 20 min. The supernatant was collected, and the protein concentration was standardized via the BCA assay. A 1:1 volume of loading buffer was added. The mixture was heated at 100 °C for 10 min, cooled, and stored at –80 °C. SDS–PAGE electrophoresis (120 V) was performed with 20 μg of protein. The gel (200 mA, 60 min) was transferred after the marker reached the bottom of the separating gel. The samples were blocked with 5% nonfat milk powder at room temperature for 1 hour. The samples were incubated overnight at 4 °C with primary antibodies against CLDN1 (Hangzhou Hua'an Biotechnology Co., Ltd., HA721999, 1:2000) and GAPDH (Wuhan Sanying Biotechnology Co., Ltd., 60004-1-Ig, 1:10000) at 4 °C. After the membranes were washed with TBST, they were incubated with secondary antibodies for 1 hour. Following another wash, the samples were visualized with an enhanced chemiluminescence (ECL) reagent. The blot bands were detected via a chemiluminescent imaging system. The target protein molecular weights were determined relative to those of the prestained marker, and quantitative analysis was performed via ImageJ (1.53e) software.

 doi:10.20944/preprints202603.0537.v1

Data Statistics and Analysis

ANOVA was performed on mucosal phenotypic characteristics using SPSS Statistics 27 software. Multiple comparisons were followed by LSD post hoc tests, with results expressed as mean±SEM. Spearman correlation analysis was performed between differential microbes, differential genes, and VFAs. Results only indicate correlations without assessing significance, with FDR controlled using Benjamini–Hochberg correction. VFAs underwent one-way ANOVA using GraphPad Prism 10.1.2, with $p < 0.05$ as the significance threshold.

Results

Effects of Different Feeding Regimens on Intestinal Barrier Integrity

H&E staining revealed changes in intestinal barrier integrity under different conditions. The CON group presented an intact colonic mucosal architecture with regularly arranged columnar epithelial cells (Figure 1A). In contrast, the HC group showed varying degrees of erosion in the colonic epithelium and muscularis, indicating that the high-concentrate diet damaged the intestinal mucosal barrier (Figure 1B). Compared with that in the HC group, the mucosal structure in the HCY group (supplemented with yeast culture) improved, with more orderly epithelial cell arrangement and reduced inflammatory infiltration, although it did not fully recover to CON levels (Figure 1C).

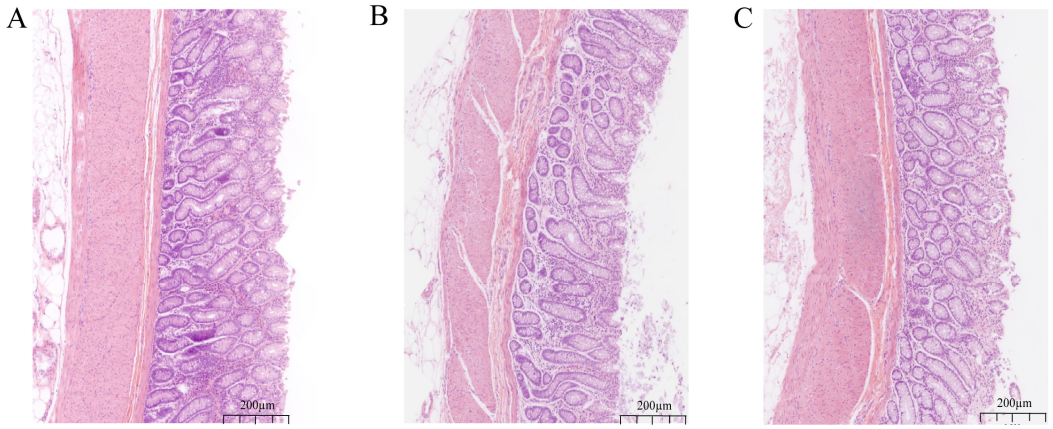

Figure 1. Effects of different diets on colonic tissue morphology in sheep. (**A**) CON: basal diet control. (**B**) HC: high-concentrate feeding. (**C**) HCY: high-concentrate diet + yeast culture feeding.

Specifically, crypt depth, muscularis thickness, and submucosal layer thickness exhibited extremely significant differences among all groups ($p < 0.01$)（Table 3）, while crypt width and myoepithelial layer thickness showed no significant changes ($p > 0.05$). Multiple comparisons revealed that compared with the CON group, both the HC and HCY groups exhibited significantly reduced crypt depth and submucosal layer thickness ($p < 0.01$), with the HCY group showing significantly higher values than the HC group. Regarding muscularis layer thickness, both the HC and HCY groups were significantly thinner than the CON group ($p < 0.01$), and no significant difference was observed between these two groups ($p > 0.05$).

Table 3. Effects of Different Diets on Sheep Colon Mucosa.

Indicators	CON	HC	HCY	P
Crypt depth (mm)	381.0896±7.1817A	218.4259±8.3947BC	322.4586±9.2712AB	<0.01
Crypt width (mm)	40.626±1.9262	36.7474±1.5182	36.8027±1.0481	0.144
Muscle layer thickness (mm)	313.4273±8.2009A	196.2983±2.9708AB	175.1622±3.6256B	<0.01

 doi:10.20944/preprints202603.0537.v1

Submucosal thickness (mm)	75.5931±1.8456A	38.9403±1.0286BC	46.7882±2.7101AB	<0.01
Serosal thickness (mm)	55.838±1.9128	52.4145±1.8280	52.8953±1.4258	0.334

[a,b,c] Values within a row with different superscripts differ significantly at P < 0.05. [A,B,C] Values within a row with different superscripts differ significantly at P < 0.01. CON: basal diet control. HC: high-concentrate feeding. HCY: high-concentrate diet + yeast culture feeding.

Changes in the Contents of Volatile Fatty Acids and Ammonia Nitrogen in the Colon

We employed one-way analysis of variance to determine the concentrations of volatile fatty acids (VFAs) (mmol/L) and ammonia nitrogen (mg/L) in the colonic contents. The results are presented in Figure 2. The HC group presented the highest ammonia nitrogen content (Figure 2A) and the lowest levels of acetate (Figure 2B), propionate (Figure 2C), butyrate (Figure 2D), and valerate (Figure 2E). In the HCY group, all VFAs increased, whereas ammonia nitrogen remained intermediate between the two groups. The acetic and propionic acid concentrations in the CON group differed significantly from those in the HC group ($p < 0.05$), whereas the differences in butyric and valeric acid concentrations were not significant ($p > 0.05$). In the HCY group, all VFAs differed significantly from those in the HC group ($p < 0.05$), and the butyric acid concentration in the CON group also differed significantly from that in the HC group ($p < 0.05$).

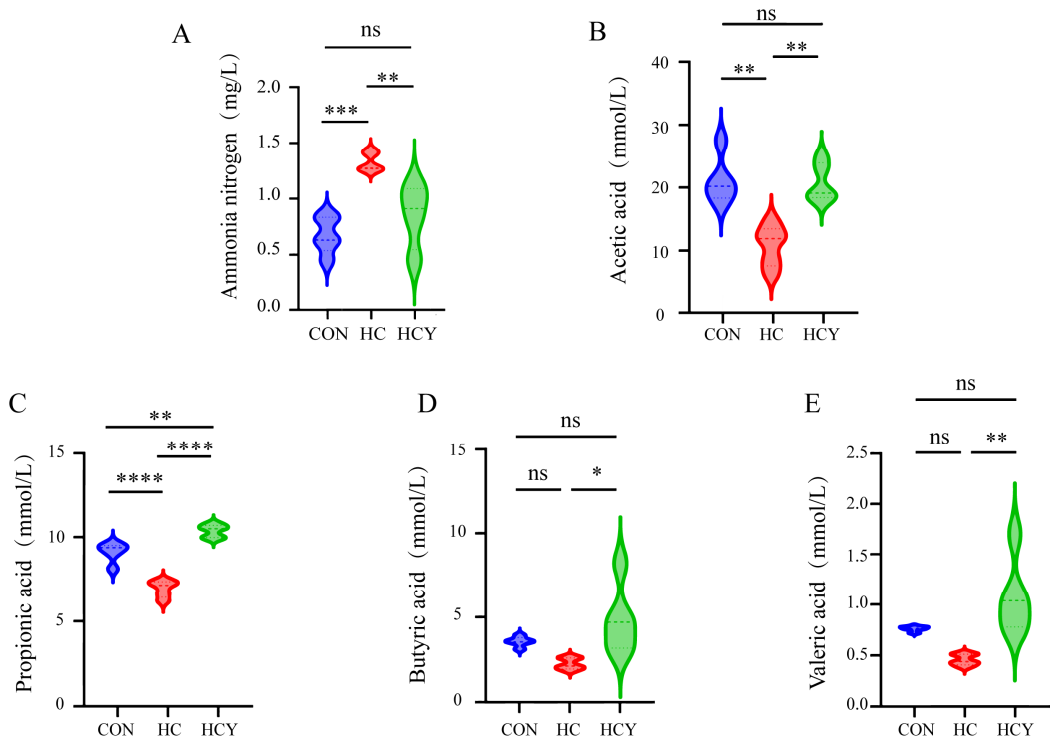

Figure 2. VFA content under different feeding conditions. (**A**) Ammonia nitrogen content in the colonic contents. (**B**) Acetic acid content in the colonic contents. (**C**) Propionic acid content in the colonic contents. (**D**) Butyric acid content in the colonic contents. (**E**) Valeric acid content in the colonic contents. Among these, no significant difference was observed (ns, $P > 0.05$); a significant difference was present (*, $P < 0.05$); and an extremely significant difference was noted (**, $P < 0.01$).

 doi:10.20944/preprints202603.0537.v1

Changes in Colonic Microbial Diversity, Composition, and Function

To assess the microbial composition, high-throughput 16S rRNA gene sequencing was performed. A total of 2,707,176 high-quality sequences were obtained. Sequences were clustered into 2,619 operational taxonomic units (OTUs), with 1,808 shared OTUs (69.03%). Additionally, 203 OTUs (7.75%) were shared exclusively between CON and HC, 186 OTUs (7.10%) were shared exclusively between CON and HCY, and 129 OTUs (4.93%) were shared exclusively between HC and HCY. Group-specific OTUs were 103 (3.93%) in the CON group, 49 (1.87%) in the HC group, and 141 (5.38%) in the HCY group. (Figure 3B). The dilution curve (Figure 3A) indicates that the sequencing depth in this study covered the vast majority of bacterial diversity within the samples, enabling a relatively comprehensive reflection of microbial community diversity. To investigate relative abundance, α-diversity (Simpson, Shannon) analysis was performed (Figure 3C,D), revealing no significant differences. However, PLS-DA analysis of β-diversity revealed significant separation between groups (Figure 3E), indicating that the presence of key bacteria exhibited significant variation. Further phylogenetic composition analysis (Figure 3F) revealed that Bacteroidetes and Firmicutes dominated at the phylum level across all three groups. At the genus level (Figure 3G), the relative abundance of Prevotella decreased in the HC group compared with the CON group. In the HCY group, the abundance of this genus significantly increased, surpassing the CON level. We subsequently performed differential species analysis via the Kruskal–Wallis test (Figure 3H), defining $P < 0.05$ as indicative of differentially abundant OTUs. The results revealed significant differences in *Cyanobacteria, Verrucomicrobiota, Ruminococcaceae;uncultured, Eubacterium_xylanophilum_group, Alistipes, Akkermansia, Gastranaerophilales,* and *Lachnospiraceae_UCG_010.* Specifically, the abundances of *Ruminococcaceae;uncultured, Akkermansia, and Verrucomicrobiota* tended to decrease across the CON, HC, and HCY groups. The abundance of the remaining taxa peaked in the HC group but decreased after YC supplementation.

On the basis of the PICRUSt2 prediction results, differential analysis of microbial functions was subsequently performed via the LEfSe method (threshold set at LDA > 2.0, $p < 0.05$). Results (Figure 3I) revealed eight significantly enriched functional pathways involving key biological processes, such as bile acid metabolism, energy supply, and DNA repair. The CON group was dominated by bile acid metabolism and butyrate metabolism pathways, whereas the HCY group was significantly enriched in DNA repair and protein secretion-related functions.

Transcriptome Analysis Indicates That Different Diets May Induce Changes in Gene Expression

To elucidate the effects of different feeding treatments on gene expression profiles in lamb colon tissue, the colonic mucosa was subjected to transcriptome sequencing. Each sample yielded approximately 16.62 Gb of raw 150-bp paired-end sequencing data. After quality control filtering and adapter removal, an average of 49.6 million high-quality clean reads were obtained per sample. Among these, 96.21% of the reads were successfully aligned to the sheep reference genome (ARS-UI_Ramb_v3.0), covering 21,473 genes. Differentially expressed genes were identified using a threshold of $|\log2FC| \geq 0.58$ and FDR-adjusted *significance* $p < 0.05$. Compared with those in the CON group, 29 genes, including 3 upregulated genes and 26 downregulated genes, were significantly differentially expressed in the colon tissue of the HC group (Figure 4A). The HCY group included 683 DEGs, comprising 264 upregulated genes and 419 downregulated genes (Figure 4A). The HC and HCY groups shared 105 differentially expressed genes, including 41 upregulated genes and 64 downregulated genes (Figure 4A). We statistically analyzed the number of DEGs and visualized their distribution across groups via a Venn diagram (Figure 4B).

KEGG pathway enrichment analysis revealed that the CON and HC groups were enriched in 6 pathways related to the immune barrier (Figure 4C); the HC and HCY groups were enriched in 22 pathways related to the immune barrier (Figure 4D); and the CON and HCY groups were enriched in 37 pathways related to the immune barrier (Figure 4E).

 doi:10.20944/preprints202603.0537.v1

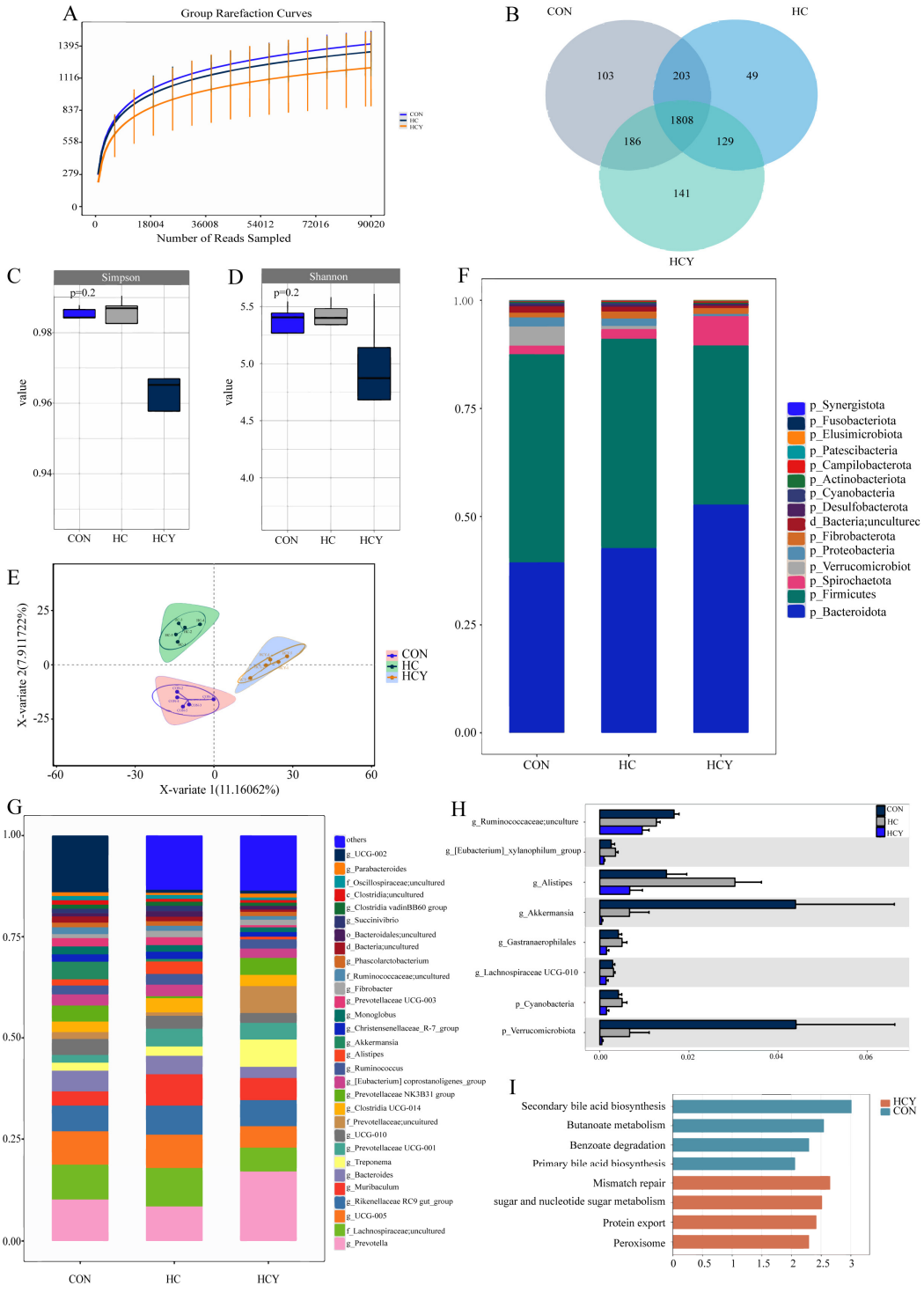

Figure 3. Effects of different feeding conditions on the microbial community of sheep. (**A**) Rarefaction curves showing the cumulative number of operational taxonomic units (OTUs) in each treatment group at different sequencing depths. (**B**) Venn diagram of OTU sharing and specificity among the three groups. (**C**) Box plot of the Simpson index. (**D**) Box plot of the Shannon index. (**E**) Two-dimensional scatter plot of partial least squares discriminant analysis (PLS-DA). (**F**) Stacked bar chart of the relative abundance of the top 15 dominant taxa at the phylum level. (**G**) Stacked bar chart of the relative abundance of the top 30 dominant taxa at the genus level. (**H**) Kruskal–Wallis method for differential species analysis at the phylum and genus levels. (**I**) LEfSe microbial KEGG functional prediction.

 doi:10.20944/preprints202603.0537.v1

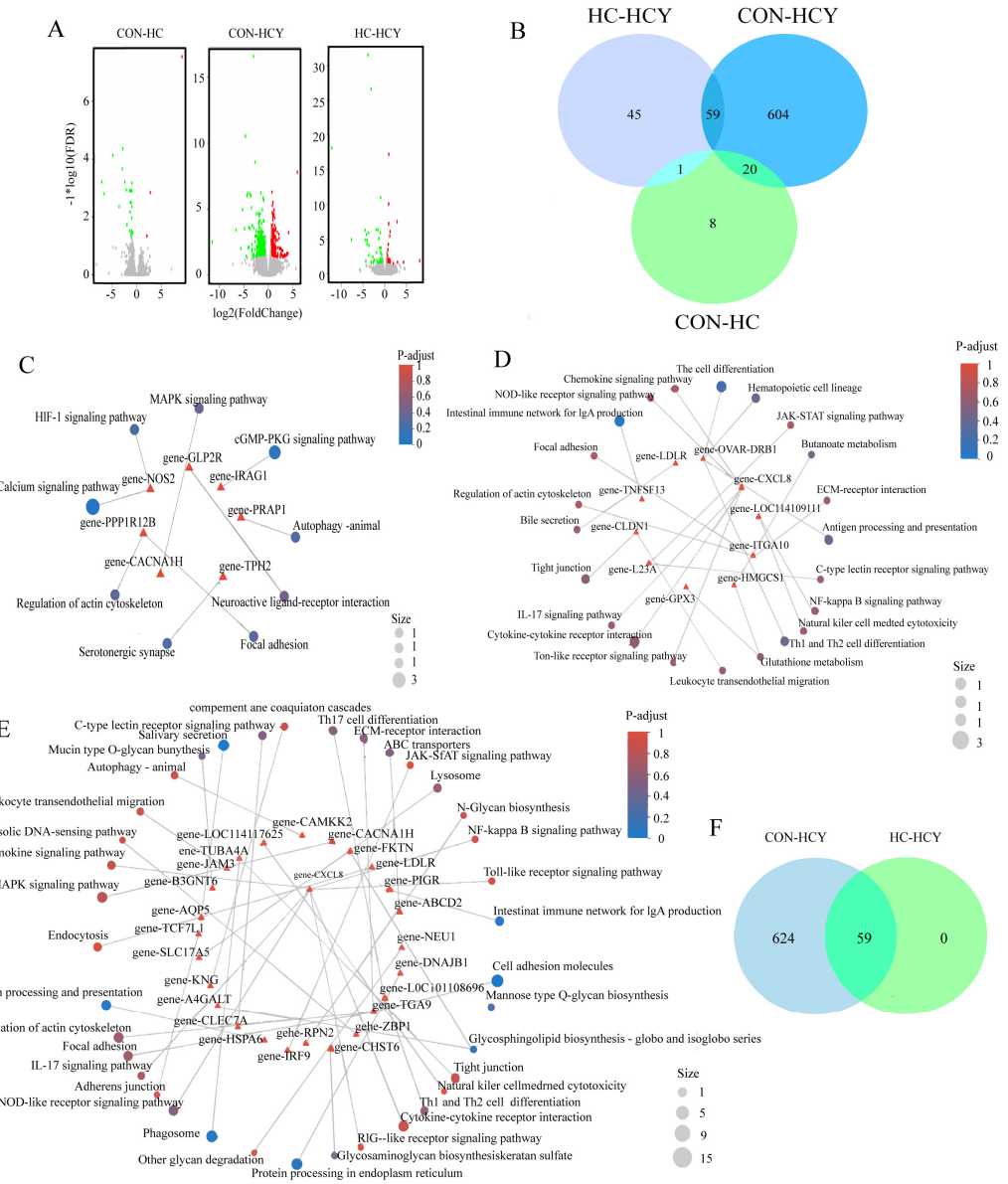

Figure 4. The influence of different feeding conditions on the transcriptome of sheep. (**A**) Volcano map of genes that were differentially expressed between groups. (**B**) Venn diagrams of differentially expressed genes in different groups. (**C**) CON-HC KEGG functional enrichment circle map of differentially expressed genes related to immune barriers. (**D**) HC-HCY KEGG functional enrichment circle map of differentially expressed genes related to immune barriers. (**E**) CON-HCY KEGG functional enrichment circle map of differentially expressed genes related to immune barriers. (**F**) Venn diagram of immune barrier-related DEGs between CON-HCY and HC-HCY.

A combined Venn diagram of the differentially expressed genes between CON-HCY and HC-HCY was constructed to identify genes specific to yeast culture treatment ($p < 0.05$). The results revealed 59 YC-specific genes, 53 of which were named. Among these genes, six were associated with the immune barrier (Figure 4F): *IL23A, ADIPOQ, CXCL8, CLDN1, TNFSF13, and Ovar-DRB1*.

Differences in the Expression of Immune Barrier-Related Genes Across Treatment Groups

Western blotting revealed reduced expression of the tight junction protein CLDN1 in the HC group of the colon, while YC treatment reversed this decrease (Figure 5A,B). However, quantitative

 doi:10.20944/preprints202603.0537.v1

analysis of the integrated gene sets via RSEM, along with qPCR validation, demonstrated that *CLDN1* was significantly upregulated in the HC group. Additionally, the qPCR results revealed that, compared with the CON group, the HCs exhibited primarily downregulation of *CXCL8*, *IL23A*, and *Ovar-DRB1*, along with upregulation of *ADIPOQ* (Figure 5D–G). In the HCY group, *ADIPOQ*, *CXCL8*, and *Ovar-DRB1* expression decreased further (Figure 5D,E,G), whereas *IL23A* expression increased (Figure 5F). These findings indicate that gene expression significantly changed in the HCY group.

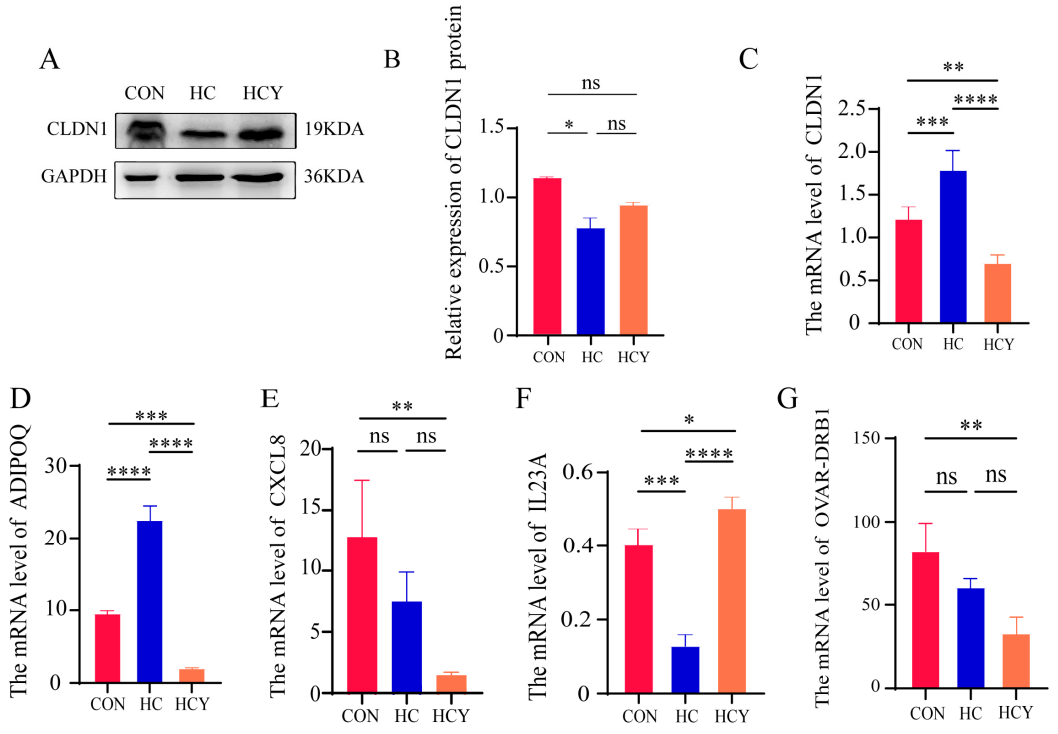

Figure 5. Effects of different diets on immune barrier genes in the colon tissue of sheep. (**A**) CLDN1 protein abundance levels in sheep colon tissue, including representative bands from Western blotting analysis and quantified volumes of specific bands. Protein expression levels were normalized against the corresponding GAPDH protein level. (**B**) CLDN1 protein expression levels in sheep colon tissue. (**C**), (**D**), (**E**), (**F**), and (**G**) Relative mRNA expression levels of *CLDN1*, *ADIPOQ*, *CXCL8*, *IL23A*, and *Ovar-DRB1* in sheep colon tissue, respectively. *GAPDH* served as the reference gene for normalization. The difference was not significant (ns, $P > 0.05$); the difference was significant (*, $P < 0.05$); the difference was extremely significant (**, $P < 0.01$).

Correlation Analysis Between the Colonic Microbiota and VFAs

We calculated Spearman's correlation coefficients, employing Benjamini–Hochberg control for FDR given the high number of parallel tests. No significant differences remained after FDR correction. Consequently, correlation analyses are presented in the main text solely as descriptive results. The findings indicate that different treatment groups (CON, HC, and HCY) presented alterations in metabolic association networks (Figure 6A). In the control group (CON), the microbiota formed stable associative patterns with VFAs. For example, *Akkermansia* and *Verrucomicrobiota* exhibited strong positive correlations with ammonia nitrogen (ρ=0.9) and a pronounced negative correlation trend with butyrate (ρ=-0.9); *Lachnospiraceae-UCG-010* showed negative correlation trends with all VFAs. Following HC treatment, the original correlation network was disrupted. Key associations in the CON group largely disappeared, with new relationships emerging: the negative correlation between *Ruminococcaceae;uncultured* and butyrate reversed to positive (ρ=0.90), whereas *Gastranaerophilales* and other taxa shifted to negative correlations with ammonia nitrogen (ρ=-0.90), indicating that HC

 doi:10.20944/preprints202603.0537.v1

treatment altered microbial metabolic functions. In the HCY group, the *[Eubacterium]-xylanophilum-group* presented extremely strong negative correlations with propionic acid and butyric acid (ϱ=-1.00; ϱ=-0.90), whereas *Ruminococcaceae;uncultured* maintained a positive correlation with valeric acid.

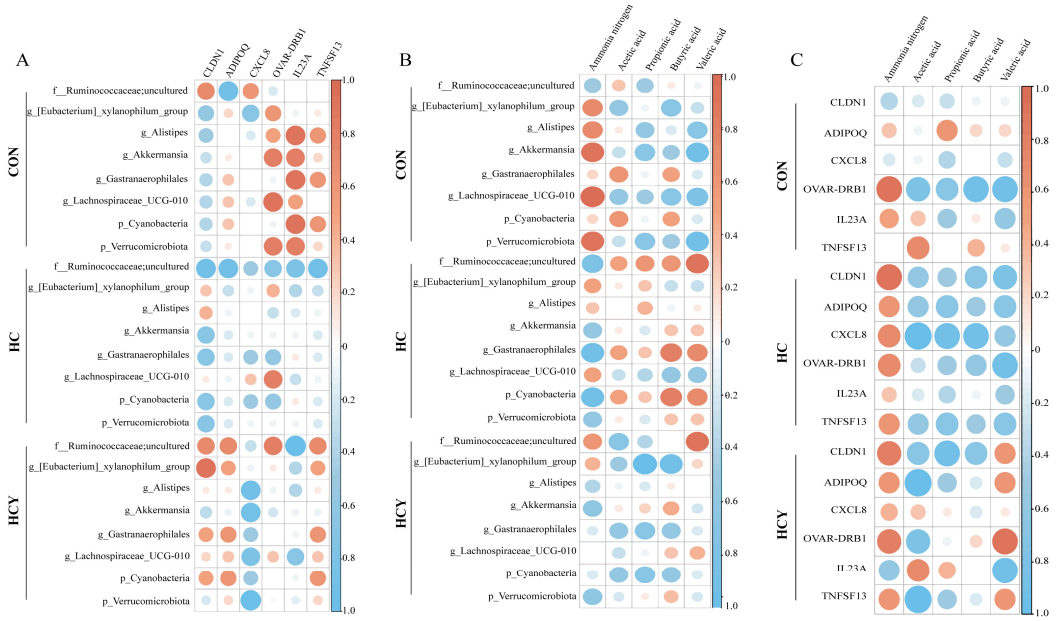

Figure 6. Heatmaps displaying Spearman's ϱ (effect sizes) only. Following FDR control (BH, 10%), no pairwise tests met the significance thresholds; thus, no significant markers are shown. (**A**) Spearman correlation analysis heatmap of differentially expressed genes related to immune barriers and differentially abundant bacteria. (**B**) Spearman correlation analysis heatmap among bacteria with differences in VFAs. (**C**) Spearman correlation analysis heatmap between VFAs and DEGs.

Correlation Analysis Between Colonic VFAs and the Transcriptome

To elucidate potential associations between host DEGs and metabolic products, Spearman correlation analyses were conducted between DEGs and VFAs (Figure 6C), and the results are presented descriptively. The findings revealed that in the CON group, *CLDN1* and *OVAR-DRB1* were negatively correlated with ammonia nitrogen, acetate, butyrate, and valerate. In the HC group, *CXCL8* was negatively correlated with acetate, propionate, and butyrate (ϱ=-1.00; ϱ=-0.90), whereas *CLDN1* was positively correlated with ammonia nitrogen (ϱ = 0.9). In the HCY group, all the negative correlations between *CXCL8* and VFAs disappeared. The negative correlation between *ADIPOQ* and *TNFSF13* with acetate increased (ϱ=-1.00), whereas the significant negative correlation between *IL23A* and valeric acid increased (ϱ=0.90). Conversely, the correlation between *OVAR-DRB1* and valeric acid shifted from negative to positive (ϱ= 0.90).

Effects of the Colonic Microbiota on Host Colonic Gene Expression Profiles

On the basis of the aforementioned DEGs and colon microbiota data, this study conducted Spearman correlation analysis (Figure 6B) to reveal host differential genes significantly associated with the gut microbiota, presenting only descriptive results. In the control group (CON), *Ruminococcaceae;uncultured* was negatively correlated with *ADIPOQ* (ϱ=-0.90), *IL23*A was positively correlated with *Alistipes, Gastranaerophilales,* and *Cyanobacteria* (ϱ=0.90), and *Ovar-DRB1* was positively correlated with *Lachnospiraceae_UCG-010* (ϱ=0.90). In the HC group, *Ruminococcaceae;uncultured* was negatively correlated with *CLDN1, ADIPOQ, and TNFSF13* (ϱ=0.90). After YC supplementation, *Ruminococcaceae;uncultured* was highly negatively correlated with *IL23A*

 doi:10.20944/preprints202603.0537.v1

(ϱ=-1.00), the *[Eubacterium]-xylanophilum-group* was positively correlated with *CLDN1* (ϱ=0.90), and *CXCL8* was negatively correlated with *Verrucomicrobiota* (ϱ=-0.98), and negatively correlated with both *Akkermansia* (ϱ=-0.89) and *Alistipes* (ϱ=0.90).

Discussion

Dietary composition differences significantly influence the sheep gut microbiota. Across dietary treatments, the gut microbial community structure, VFA profiles, and host gene expression patterns presented overall similarity, yet specific bacterial abundances, VFA levels, and related gene expression levels presented variations. This study investigated how different diets affect the colonic microbiota, VFAs, and host genes and the interrelationships among these three components.

We observed that the high-concentrate diet disrupted the integrity of the colonic mucosal barrier, whereas the YC intervention had protective and regulatory effects on the barrier. Consistent with previous studies [12], the high-concentrate diet allowed undigested starch and rapidly fermentable substrates to enter the hindgut, causing a decrease in pH, transient VFA accumulation, and osmotic pressure changes. This leads to disrupted epithelial tight junctions, goblet cell depletion, and increased local inflammation, ultimately manifesting as histological mucosal epithelial damage [13].

This study characterized the microbiota via 16S rRNA sequencing combined with functional prediction, revealing substantial microbial shifts. The *[Eubacterium]-xylanophilum group, Lachnospiraceae* and *Ruminococcaceae* have been repeatedly identified as important butyrate producers, positively correlated with barrier homeostasis [14]. Our functional predictions yielded similar results: the CON group was enriched in bile acid metabolism and butyrate metabolism, whereas the HCY group was enriched in DNA repair and protein secretion-related functions. Following injury, the intestinal epithelium requires the DNA damage response, repair, and re-epithelialization to restore barrier integrity. Furthermore, bacterial secreted proteins and exosomes interact with host receptors to regulate tight junctions and immune signaling, forming a close link with HCY group enrichment in protein secretion-related functions [15].

Microbial alterations indicate corresponding metabolic shifts, prompting us to analyze their metabolites: VFAs and ammonia nitrogen. VFAs serve as the primary energy source for ruminants, whose composition is largely influenced by feed composition [16]. Changes in ammonia nitrogen levels reflect variations in feed protein degradation efficiency and microbial activity [17]. In this study, the HC group presented the lowest VFA concentration in the colonic contents and the highest ammonia nitrogen (NH_3-N) content. This finding indicates that during hindgut fermentation, the intake of a high-concentrate diet promotes the proliferation of lactic acid bacteria, creating an acidic environment that inhibits microorganisms from utilizing lactic acid to produce butyric acid and propionic acid [8]. Additionally, protein fermentation generates ammonia and amines [18]. The HCY group presented significantly elevated acetate, propionate, butyrate, and valerate ($P < 0.05$), which is consistent with the metabolic regulatory function of YC [8]. Studies indicate that yeast culture enhances microbial nitrogen assimilation, increasing VFAs while reducing ruminal ammonia [19]. Overall, feeding a high-concentrate diet alone may reduce colonic fermentation efficiency, whereas adding yeast culture can rebalance microbial activity to increase VFAs and suppress excessive ammonia production, a trend broadly consistent with prior research [19,20]. Severe or prolonged high-concentrate feeding disrupts fiber fermentation, leading to reduced VFAs and increased proteolytic end products [21].

Our analysis of the DuHan F1 colon transcriptome revealed substantial changes in DEGs In the HCY group, indicating extensive transcriptional reprogramming. This finding aligns with previous reports in ruminant high-concentrate diet models [13]. When performing WB and qPCR for the barrier protein CLDN1, we observed inconsistent expression patterns between transcript and protein abundance. We hypothesize that this discrepancy may stem from endoplasmic reticulum stress and the inflammatory environment induced by the HC diet, which accelerates the turnover and degradation of tight junction proteins via the endocytosis-lysosomal pathway [22,23]. Concurrently,

 doi:10.20944/preprints202603.0537.v1

the mucosal epithelium may transcritionally *upregulate CLDN1* as a compensatory response, leading to a discordant pattern of increased mRNA but decreased protein levels. This process may be further promoted by E3 ubiquitin ligases (e.g., LNX1), which mediate endocytosis and subsequent lysosomal degradation of claudins—a mechanism validated across diverse epithelial cell types [23–25]. Moreover, under inflammatory conditions or upon stimulation by acidic loads or toxic metabolites, the UPR/ISR (PERK–eIF2α) pathway is readily activated, leading to a global reduction in protein translation. This results in increased transcription but restricted protein synthesis, with translation being suppressed [26,27]. In the HC group, *IL-8*, *IL-23A*, and *Ovar-DRB1* were downregulated, whereas *ADIPOQ* was upregulated. A literature review indicated that decreased *IL-8* aligns with subsequent YC-mediated suppression, which is consistent with probiotic yeast classic NF-κB inhibition [28].

Given sample size constraints and multiple corrections, correlations are presented as exploratory findings. Overall, in the CON group, VFAs were negatively correlated with proinflammatory factors (e.g., *CXCL8*), which is consistent with the anti-inflammatory regulation by SCFAs, particularly butyrate [29,30]. Concurrently, tissue damage and reduced immune cell counts induced by HC also decrease the overall expression of these immune genes [31]. Tao et al. similarly reported that a high-concentrate diet significantly downregulated the expression of proinflammatory factors such as *IL-1β* [32]. VFAs can also limit *IL-23* production by dendritic cells to regulate immunity [33]; conversely, 65% grain intake downregulates tight junction proteins, causing epithelial damage accompanied by local inflammation [34]. Under high-concentrate diet conditions, these patterns exhibited diet-dependent rearrangements with partial directional reversals (e.g., barrier-related genes and ammonia nitrogen showed parallel trends), suggesting potential limitations in VFA absorption or utilization during inflammation. YC supplementation stabilized the overall pattern: the negative coupling between VFAs and inflammation weakened, whereas the positive coupling between barrier-related indicators and key metabolites strengthened.

The microbiota strongly influences the diet and is closely associated with VFAs [35,36]. Correlations are presented as exploratory patterns. The CON group maintains a healthy fermentation network in which dominant symbionts efficiently convert fibers into short-chain fatty acids [14,37]. However, the consumption of a high-concentrate diet disrupts this equilibrium. Microorganisms associated with fiber fermentation show weakened or absent links to VFAs, whereas novel abnormal associations emerge. This finding aligns with the finding that HC inhibits normal fiber fermentation pathways and reduces fiber-degrading bacteria in the hindgut [38]. Certain rumenobacteria within the family Ruminococcaceae shift their metabolic function toward producing or tolerating valeric acid under high-concentrate diet conditions. When the abundance of fiber-degrading bacteria decreases, ammonia-producing proteolytic bacteria may proliferate substantially. The addition of YC partially restored the stability of microbial–host metabolic interactions. The abundance of the *[Eubacterium]-xylanophilum-group* was strongly negatively correlated with propionic acid (ρ = -1.00) and butyric acid (ρ = -0.90) contents. This likely reflects functional redistribution and suppression of specific acid-producing pathways following improved colonic digestion and controlled nutrient overflow [39].

Under normal conditions, host mucosal gene expression exhibits is well-coordinated regulation with the microbial community. However, diet-dependent rearrangements emerged following high-concentrate diet feeding. In the HC group, the abundance *of Ruminococcaceae;uncultured* bacteria was negatively correlated with *CLDN1, ADIPOQ, and TNFSF13*, whereas these associations were either absent or extremely weak in the CON group. This pattern aligns with reported HC-associated barrier stress/inflammatory stress [40] and is consistent with transcriptional compensation and metabolic environment alterations under stress. In the HCY group, *[Eubacterium]-xylanophilum-group* abundance was positively correlated with *CLDN1* expression (ρ=0.90), but exhibited enhanced inverse coupling with inflammatory factors (e.*g.*, *IL23A*). This aligns with the anti-inflammatory and barrier-supporting effects of the SCFA–GPR41 and GPR43 axes documented in the literature [14].

 doi:10.20944/preprints202603.0537.v1

We propose that YC primarily functions as a microbial regulator, fostering a community structure more conducive to glycolytic fermentation. This is evidenced by YC-induced inhibition of certain bacteria and promotion of a metabolic environment characterized by increased VFA production and reduced ammonia nitrogen content. The re-regulated microbial-metabolite interactions subsequently create a favorable environment for the host mucosa. This hypothesis is supported by our observed correlation analysis: the rebound of VFAs following YC supplementation correlates with the normalization of immune gene expression (e.g., downregulation of *CXCL8* and *ADIPOQ*) and the restoration of CLDN1 protein abundance. However, this study has certain limitations. Particularly in metabolite analysis, it focused solely on changes in VFAs (acetic, propionic, butyric, and valeric acids), failing to comprehensively assess whether other metabolites were affected by the high-concentrate diet and YC intervention. It lacked broader metabolomics and causal validation, and the small sample size precludes causal discussions. Therefore, future studies should employ larger sample sizes under different dietary interventions and utilize metabolomics or metagenomics to further investigate the interactions among colonic metabolites, microbial communities, and host health in sheep.

Conclusions

This study investigated the differential effects of different diets on the colon and the regulatory mechanisms of YC through a multi-omics analysis integrating sheep colon morphology, microbial communities, VFAs, and gene expression. Results indicate that the high-concentrate diet caused damage to colonic mucosal architecture, reduced crypt depth and submucosal thickness, accompanied by decreased volatile fatty acids and elevated ammonia nitrogen, disrupting hindgut fermentation patterns. Yeast culture re-regulated this network, restoring VFA levels and lowering ammonia nitrogen concentrations. Elevated VFA content and reduced ammonia nitrogen were observed, along with altered expression of immune-related genes such as *CLDN1*, *CXCL8*, and *IL23A*. Collectively, yeast culture modulates changes in the intestinal environment induced by high-concentrate diets by regulating interactions among gut microbiota, metabolites, and host immune barrier-related genes. These findings provide a theoretical foundation for nutritional management in ruminants and support the development of more precise probiotic formulations.

Conflicts of Interest: The authors declare that the research was conducted in the absence of any commercial or financial relationships that could be construed as a potential conflict of interest.

Authors' Contribution: Data curation: Li HK, Niu MQ, Yang FF, Pi ZW. Formal analysis: Li HK. Methodology: Li HK, Tang ZX, Yang FF, Pi ZW. Software: Li HK, Yang FF. Validation: Li HK, Yang FF, Pi ZW. Investigation: Li HK. Writing - original draft: Li HK. Writing - review & editing: Li HK, Cheng SR, Niu MQ, Shi JP, Tang ZX, Yang FF, Pi ZW.

Funding: This research was supported by the National Natural Science Foundation of China (Project No.32460824).

Acknowledgments: We acknowledge the support provided by the College of Animal Science and Technology at Gansu Agricultural University for this research.

Data Availability: The sequencing data have been uploaded to the SRA database at the NCBI Data Centre, with the biological accession number PRJNA1329256.

Ethics Approval: All animal procedures used in this study were approved by the Institutional Animal Care and Use Committee of Gansu Agricultural University (Certification Number: GSAU-Eth-AEW-2024-032).

Declaration of Generative AI: No AI tools were used in this article.

 doi:10.20944/preprints202603.0537.v1

References

1. Lu Z, Kong L, Ren S, et al.Acid tolerance of lactate-utilizing bacteria of the order Bacteroidales contributes to prevention of ruminal acidosis in goats adapted to a high-concentrate diet.Animal Nutrition.2023;14:130-140.https://doi.org/10.1016/j.aninu.2023.05.006.
2. Gressley T, Hall M, Armentano L J J o a s.Ruminant nutrition symposium: productivity, digestion, and health responses to hindgut acidosis in ruminants.J Anim Sci.2011;89:1120-1130.https://doi.org/10.2527/jas.2010-3460.
3. Zeng J, Lv J, Duan H, et al.Subacute Ruminal Acidosis as a Potential Factor that Induces Endometrium Injury in Sheep.Int J Mol Sci.2023;24.https://doi.org/10.3390/ijms24021192.
4. Fu R, Liang C, Chen D, et al.Yeast hydrolysate attenuates lipopolysaccharide-induced inflammatory responses and intestinal barrier damage in weaned piglets.J Anim Sci Biotechnol.2023;14:44.https://doi.org/10.1186/s40104-023-00835-2.
5. Váradyová Z, Zeleňák I, Siroka P J A f s, et al.In vitro study of the rumen and hindgut fermentation of fibrous materials (meadow hay, beech sawdust, wheat straw) in sheep.2000;83:127-138
6. Yan S, Du R, Yao W, et al.Host–microbe interaction-mediated resistance to DSS-induced inflammatory enteritis in sheep.Microbiome.2024;12:208.https://doi.org/10.1186/s40168-024-01932-8.
7. Jin C, Wu S, Liang Z, et al.Multi-omics reveal mechanisms of high enteral starch diet mediated colonic dysbiosis via microbiome-host interactions in young ruminant.Microbiome.2024;12:38.https://doi.org/10.1186/s40168-024-01760-w.
8. Wang H, Liu G, Zhou A, et al.Effects of yeast culture on in vitro ruminal fermentation and microbial community of high concentrate diet in sheep.AMB Express.2024;14:37.https://doi.org/10.1186/s13568-024-01692-6.
9. Wang X, Li F, Zhang N, et al.Effects of supplementing a yeast culture in a pelleted total mixed ration on fiber degradation, fermentation parameters, and the bacterial community in the rumen of sheep.Anim Feed Sci Technol.2023;296:115565.https://doi.org/10.1016/j.anifeedsci.2022.115565.
10. Chen H, Liu S, Li S, et al.Effects of yeast culture on growth performance, immune function, antioxidant capacity and hormonal profile in Mongolian ram lambs.Front Vet Sci.2024;11:1424073.https://doi.org/10.3389/fvets.2024.1424073.
11. Amin A B, Mao S.Influence of yeast on rumen fermentation, growth performance and quality of products in ruminants: A review.Anim Nutr.2021;7:31-41.https://doi.org/10.1016/j.aninu.2020.10.005.
12. Ye H, Liu J, Feng P, et al.Grain-rich diets altered the colonic fermentation and mucosa-associated bacterial communities and induced mucosal injuries in goats.Sci Rep.2016;6:20329.https://doi.org/10.1038/srep20329.
13. Wang Y, Xu L, Liu J, et al.A High Grain Diet Dynamically Shifted the Composition of Mucosa-Associated Microbiota and Induced Mucosal Injuries in the Colon of Sheep.Front Microbiol.2017;8:2080.https://doi.org/10.3389/fmicb.2017.02080.
14. Wei J, Zhao Y, Zhou C, et al.Dietary Polysaccharide from Enteromorpha clathrata Attenuates Obesity and Increases the Intestinal Abundance of Butyrate-Producing Bacterium, Eubacterium xylanophilum, in Mice Fed a High-Fat Diet.Polymers (Basel).2021;13.https://doi.org/10.3390/polym13193286.
15. Balint D, Brito I L.Human-gut bacterial protein-protein interactions: understudied but impactful to human health.Trends Microbiol.2024;32:325-332.https://doi.org/10.1016/j.tim.2023.09.009.
16. Sutton J D, Dhanoa M S, Morant S V, et al.Rates of Production of Acetate, Propionate, and Butyrate in the Rumen of Lactating Dairy Cows Given Normal and Low-Roughage Diets.J Dairy Sci.2003;86:3620-3633.https://doi.org/10.3168/jds.S0022-0302(03)73968-X.
17. Grummer R R, Clark J H, Davis C L, et al.Effect of ruminal ammonia-nitrogen concentration on protein degradation in situ.J Dairy Sci.1984;67:2294-2301.https://doi.org/10.3168/jds.S0022-0302(84)81577-5.
18. Zhang K, Xu Y, Yang Y, et al.Gut microbiota-derived metabolites contribute negatively to hindgut barrier function development at the early weaning goat model.Anim Nutr.2022;10:111-123.https://doi.org/10.1016/j.aninu.2022.04.004.
19. Garcia Diaz T, Ferriani Branco A, Jacovaci F A, et al.Inclusion of live yeast and mannan-oligosaccharides in high grain-based diets for sheep: Ruminal parameters, inflammatory response and rumen morphology.PLoS One.2018;13:e0193313.https://doi.org/10.1371/journal.pone.0193313.

 doi:10.20944/preprints202603.0537.v1

20. Alshaikh M, Alsiadi M Y, Zahran S, et al.Effect of Feeding Yeast Culture from Different Sources on the Performance of Lactating Holstein Cows in Saudi Arabia.J Anim Sci.2002;15:352-356.https://doi.org/10.5713/ajas.2002.352.
21. Hao Y, Ouyang T, Wang W, et al.Competitive Analysis of Rumen and Hindgut Microbiota Composition and Fermentation Function in Diarrheic and Non-Diarrheic Postpartum Dairy Cows.Microorganisms.2024;12:23.https://doi.org/10.3390/microorganisms12010023.
22. Luissint A-C, Parkos C A, Nusrat A.Inflammation and the Intestinal Barrier: Leukocyte–Epithelial Cell Interactions, Cell Junction Remodeling, and Mucosal Repair.Gastroenterology.2016;151:616-632.https://doi.org/10.1053/j.gastro.2016.07.008.
23. Stamatovic S M, Johnson A M, Sladojevic N, et al.Endocytosis of tight junction proteins and the regulation of degradation and recycling.Ann N Y Acad Sci.2017;1397:54-65.https://doi.org/10.1111/nyas.13346.
24. Takahashi S, Iwamoto N, Sasaki H, et al.The E3 ubiquitin ligase LNX1p80 promotes the removal of claudins from tight junctions in MDCK cells.J Cell Sci.2009;122:985-994.https://doi.org/10.1242/jcs.040055.
25. Cai J, Culley M K, Zhao Y, et al.The role of ubiquitination and deubiquitination in the regulation of cell junctions.Protein Cell.2018;9:754-769.https://doi.org/10.1007/s13238-017-0486-3.
26. Wek R C.Role of eIF2α Kinases in Translational Control and Adaptation to Cellular Stress.Cold Spring Harb Perspect Biol.2018;10.https://doi.org/10.1101/cshperspect.a032870.
27. Eugene S P, Reddy V S, Trinath J.Endoplasmic Reticulum Stress and Intestinal Inflammation: A Perilous Union.Front Immunol.2020;Volume 11 - 2020:
28. Pothoulakis C.Review article: anti-inflammatory mechanisms of action of Saccharomyces boulardii.Aliment Pharmacol Ther.2009;30:826-833.https://doi.org/10.1111/j.1365-2036.2009.04102.x.
29. Diao H, Jiao A R, Yu B, et al.Gastric infusion of short-chain fatty acids can improve intestinal barrier function in weaned piglets.Genes Nutr.2019;14:4.https://doi.org/10.1186/s12263-019-0626-x.
30. Siddiqui M T, Cresci G A M.The Immunomodulatory Functions of Butyrate.J Inflamm Res.2021;14:6025-6041.https://doi.org/10.2147/jir.S300989.
31. Savidge T C, Newman P G, Pan W-H, et al.Lipopolysaccharide-Induced Human Enterocyte Tolerance to Cytokine-Mediated Interleukin-8 Production May Occur Independently of TLR-4/MD-2 Signaling.Pediatric Research.2006;59:89-95.https://doi.org/10.1203/01.pdr.0000195101.74184.e3.
32. Tao S, Duanmu Y, Dong H, et al.High Concentrate Diet Induced Mucosal Injuries by Enhancing Epithelial Apoptosis and Inflammatory Response in the Hindgut of Goats.PLoS One.2014;9:e111596.https://doi.org/10.1371/journal.pone.0111596.
33. Nastasi C, Fredholm S, Willerslev-Olsen A, et al.Butyrate and propionate inhibit antigen-specific CD8+ T cell activation by suppressing IL-12 production by antigen-presenting cells.Scientific Reports.2017;7:14516.https://doi.org/10.1038/s41598-017-15099-w.
34. Liu J H, Xu T T, Liu Y J, et al.A high-grain diet causes massive disruption of ruminal epithelial tight junctions in goats.Am J Physiol Regul Integr Comp Physiol.2013;305:R232-241.https://doi.org/10.1152/ajpregu.00068.2013.
35. Jing X P, Zhao L, Wang W J, et al.Effects of dietary energy levels on production and absorption of hindgut short-chain fatty acids in two sheep breeds.Animal.2025;19:101447.https://doi.org/10.1016/j.animal.2025.101447.
36. Siciliano-Jones J, Murphy M R.Production of volatile fatty acids in the rumen and cecum-colon of steers as affected by forage:concentrate and forage physical form.J Dairy Sci.1989;72:485-492.https://doi.org/10.3168/jds.S0022-0302(89)79130-X.
37. Mukherjee A, Lordan C, Ross R P, et al.Gut microbes from the phylogenetically diverse genus Eubacterium and their various contributions to gut health.Gut Microbes.2020;12:1802866.https://doi.org/10.1080/19490976.2020.1802866.
38. Zhang R, Liu J, Jiang L, et al.The Remodeling Effects of High-Concentrate Diets on Microbial Composition and Function in the Hindgut of Dairy Cows.Front Nutr.2022;Volume 8 - 2021.https://doi.org/10.3389/fnut.2021.809406.

 doi:10.20944/preprints202603.0537.v1

39. Jouany J P, Medina B, Bertin G, et al.Effect of live yeast culture supplementation on hindgut microbial communities and their polysaccharidase and glycoside hydrolase activities in horses fed a high-fiber or high-starch diet.J Anim Sci.2009;87:2844-2852.https://doi.org/10.2527/jas.2008-1602.
40. Tao S, Duanmu Y, Dong H, et al.A high-concentrate diet induced colonic epithelial barrier disruption is associated with the activating of cell apoptosis in lactating goats.BMC Vet Res.2014;10:235.https://doi.org/10.1186/s12917-014-0235-2.